Journal of Power Sources 271 (2014) 326–333

Contents lists available at ScienceDirect

Journal of Power Sources

journal homepage: www.elsevier.com/locate/jpowsour

Activated oil sands fluid coke for electrical double-layer capacitors

Jocelyn E. Zuliani [a], Donald W. Kirk [a], Charles Q. Jia [a, *], Shitang Tong [b]

[a] Department of Chemical Engineering & Applied Chemistry, University of Toronto, 200 College St., Toronto, Ontario M5S 3E5, Canada
[b] Department of Chemical Engineering, Wuhan University of Science and Technology, 947 Heping Avenue, Wuhan, Hubei 430081, China

HIGHLIGHTS

- High-sulphur oil sands fluid coke is used to form high surface area porous carbon.
- Activated fluid coke is used as electrode material in an electrochemical capacitor.
- High capacitance (190 F g^{-1}) is achieved at fast charging rates (7.5 A g^{-1}).
- Fluid coke's unique layered structure may enhance ion transport and its performance.
- Sulphur in the activated fluid coke may enhance energy storage.

GRAPHICAL ABSTRACT

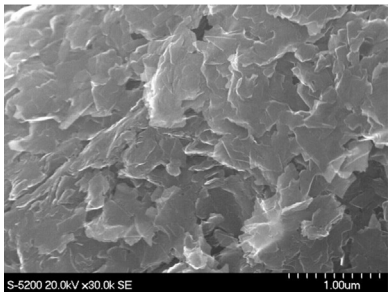

ARTICLE INFO

Article history:
Received 27 February 2014
Received in revised form
3 July 2014
Accepted 26 July 2014
Available online 4 August 2014

Keywords:
Electrochemical capacitors
Oil sands fluid coke
Porous carbon electrodes
Energy storage
Concentric layered structure
Organic sulphur

ABSTRACT

Electrochemical capacitors are important energy storage devices that have high power density, rapid charging cycles and are highly cyclable. In this study, activated fluid coke has demonstrated high surface area, improved capacitive properties, and high energy density. Fluid coke is a by-product generated from continuous high temperature bitumen upgrading, resulting in the formation of nearly spherical particles with concentric carbon layers. The residual sulphur impurities in fluid coke may enhance its energy storage performance. The activated coke samples have high specific surface areas, up to 1960 m^2 g^{-1}, and show promising capacitive performance, in 4 M KOH electrolyte, with high gravimetric and specific capacitances of 228–257 F g^{-1} and 13–14 μF cm^{-2}, respectively. These results are comparable to other top performing activated carbon materials [1–3]. The activated fluid coke maintains high performance at fast charging rates, greater than 160 F g^{-1} at a current density of 7500 mA g^{-1}. Activated fluid coke's high capacitance and promising rate performance are potentially associated with its unique layered, and the moderate sulphur content in the chemical structure. Activated fluid coke is a unique opportunity to use a limited use by-product to generate activated carbon that has a high surface area and promising energy storage properties.

1. Introduction

Electrical double-layer capacitors (EDLCs) are developing electrical energy storage devices that have shown promise to bridge the energy and power gap between traditional batteries and electrostatic capacitors [4]. Though the energy density of EDLCs is less than batteries, EDLCs have demonstrated a high power density, long lifetimes and cyclability, and rapid charging cycles. Energy is stored in EDLC devices by charging the electrical double layer. Charging occurs when electrolyte ions adsorb onto the surface of a porous electrode, thereby making the process rapid and highly reversible. In contrast to batteries, which require rare metallic

* Corresponding author. Tel.: +1 416 946 3097; fax: +1 416 978 8605.
E-mail address: cq.jia@utoronto.ca (C.Q. Jia).

http://dx.doi.org/10.1016/j.jpowsour.2014.07.171
0378-7753/

compounds (such as cobalt in lithium batteries) for the electrodes, EDLCs use abundantly available carbon as the electrode material [1,4–6]. There are two key electrochemical components in EDLCs: the electrode material and the electrolyte. In this study, an aqueous solution of 4 M potassium hydroxide is used as the electrolyte. Aqueous electrolytes have a limited voltage window, due to the electrolytic decomposition of water; however, they offer the benefits of high conductivity, high dielectric constants, and smaller ions, which all increase the potential capacitance [5,7].

The electrode material is an important consideration for EDLC design. Several materials are being investigated for EDLC electrodes including carbon nanotubes (CNTs), template carbons, graphene sheets, and carbide-derived carbons [1,8–11]; however, many of these carbon sources require complex preparation methods that result in increased production costs. In general, nanomaterials, such as graphene and CNTs, are highly desirable for ion adsorption applications due to the high electrical conductivity, the ordered structure, and the high surface area to volume. However, the performance of these materials requires meticulous preparation techniques due to the difficulty in overcoming the strong intermolecular attractions, which cause agglomeration. Multi-wall carbon nanotubes have shown a range in capacitance, on a per unit weight basis, of between 20 F g^{-1} to 207 F g^{-1} when using aqueous potassium hydroxide as the electrolyte [11]. One of the main challenges associated with CNTs is creating the ordered structure needed to maximize the ion accessible surface area, due to the strong van der Waals forces between the CNTs. However, if the CNTs can be grown vertically, in an ordered structure, the high electrical conductivity, and accessible surface area allow for high charging currents, up to 10 A g^{-1} [1].

Researchers investigating graphene nanoparticles and nanosheets have also shown a range of gravimetric capacitance values between 120 and 397 F g^{-1}, in an aqueous potassium hydroxide electrolyte. Again, the performance of these materials is heavily dependent on the preparation technique employed. Graphene based supercapacitors have a sharp increase in capacitance at low charging rates and have been shown to maintain a high performance at very fast charging rates, up to 20 A g^{-1} and 500 mV s^{-1} [11–14].

Activated carbon (AC) is an emerging EDLC electrode material that is demonstrating promising performance due to its high specific surface area (SSA), high electrical conductivity, good chemical stability, and relatively low cost [1,4] when compared to the more exotic nanomaterials discussed above. Activated carbon electrodes typically have high capacitance values on a per unit weight basis due to high porosity and surface area. Typically the gravimetric capacitance of AC electrodes ranges between 50 F g^{-1} to 250 F g^{-1}; however, some researchers have demonstrated higher capacitance values, up to 400 F g^{-1} [1,2,15,16].

Activated carbon electrodes tend to have moderate specific capacitance values as a result of limited ion access to the total measurable surface area [5–7]. The specific capacitance values tend to range between, 8–11 μF cm^{-2} [1,2,15,16] which are below the generally accepted maximum specific capacitance of carbon materials, estimated to be 21 μF cm^{-2} for a graphene sheet [17]. One of the highest reported specific capacitance values is activated mesocarbon beads with a specific capacitance of 19.1 μF cm^{-2} (275 F g^{-1}), for an AC material that has a surface area of 1443 m^2 g^{-1} [2]. Other researchers have reported specific capacitance values well above the theoretical limit of carbon; however, these elevated capacitance values are often associated with surface Faradaic reactions that will lead to an apparent enhancement in energy storage.

This study focuses on the electrochemical performance of AC materials prepared from oil sands fluid coke (OSFC): a waste by-product generated from bitumen refining process in the Alberta Oil Sands. The performance of the activated oil sands fluid coke (AFC) samples will be compared to commercially available coconut shell-derived AC (CSAC) in order to determine its electrical performance in aqueous 4 M potassium hydroxide electrolyte.

Two of the main factors that are considered in evaluating the potential of these AFC electrode materials: 1) the maximum capacitance observed at slow charging rates, and 2) the decrease in capacitance as the charging rate is increased. Ideally EDLCs should retain a large portion of its maximum capacitance at a fast charging rate: this relationship is governed by equivalent series resistance losses and ion diffusion resistance, relating to transport in the AC's confined porous network [5].

2. Experimental

2.1. Oil sands fluid petroleum coke

The Alberta Oil Sands, located in Northern Alberta, upgrade bitumen to synthetic crude oil, generating OSFC as a by-product. Fluid coking is a continuous bitumen upgrading process that cracks the bitumen over a fixed bed of fluid coke particles. During upgrading, the coke particles are recycled through the “coker” several times. The fluid coking process leads to the formation of nearly spherical particles with concentric carbon layers [18]. The OSFC is primarily composed of carbon; however, it also contains various impurities that are extracted from the bitumen during upgrading. Furmisky estimated that OSFC fluid coke is approximately 80–83 wt.% carbon, with approximately 6–7 wt.% sulphur and 5–8 wt.% oxidized ash content [19]. Due to the high sulphur content, OSFC has limited use as an energy source. Combustion of OSFC would produce significant amounts of sulphur dioxide which would require an extensive scrubber system to desulphurize the flue gas stream. Given the expense associated with SO_2 scrubbing, petroleum coke is often stockpiled as a limited use product; approximately 76 million tonnes of coke are estimated to be stockpiled to date [20].

The high carbon content of OSFC has been shown to be advantageous for generation of AC, allowing for elimination of the carbonization step – normally required for biomass-derived AC [18,21–23]. As well, the high temperature coking process results in the formation of a highly graphitized carbon material which leads to improved material conductivity [18].

2.2. Activated carbon preparation

Raw OSFC was activated using potassium hydroxide (KOH) in a tubular furnace under an inert nitrogen atmosphere. The OSFC was soaked with solid KOH, 1 mL of water per 5 g of OSFC, and 0.25 g of methanol in a steel tube reactor. After soaking, the OSFC was activated using various conditions listed in Table 1. Residual KOH was removed from the AFC samples by washing with distilled water and neutralization using dilute hydrochloric acid.

Table 1
Activation conditions for preparation of activated oil sands fluid coke.

Sample	AFC-1	AFC-2	AFC-3	AFC-4
Weight ratio (KOH:Coke)	2.5:1	2.5:1	2.5:1	2.5:1
Room temperature soaking time	90 min	30 min	19.5 h	19.5 h
Melting temperature and time	350 °C 60 min	400 °C 60 min	400 °C 120 min	400 °C 120 min
Pyrolysis temperature and time	850 °C 120 min	850 °C 120 min	850 °C 120 min	900 °C 120 min

2.3. Activated carbon characterization

The specific surface area and pore size distribution of the AFC samples were characterized using isothermal nitrogen adsorption and also with carbon dioxide adsorption to measure pores with a diameter of 0.3 nm and greater. Non-local density functional theory (NL-DFT) was used to analyze the CO_2 adsorption isotherm for pores with diameters less than 1 nm and quenched solid density functional theory (QS-DFT) was used to analyze the N_2 adsorption isotherm for pores with diameters greater than 1 nm. This analysis was similar to procedures used by Caguiat et al. to measure the surface area of nanoporous carbon materials [24].

Scanning electron microscopy (SEM) imaging of the fluid coke particles was performed using a Hitachi S-5200 scanning electron microscope. The microstructures of the material were imaged at an acceleration of 5 kV and 20 kV. The elemental composition of the AC samples was determined using the Exeter Analytical Inc., CE-440 Elemental Analyzer for carbon, hydrogen, sulphur and nitrogen.

2.4. Electrochemical performance

Two types of AC electrodes were investigated in this work, electrodes prepared using commercial CSAC, as supplied by Fisher Scientific, and electrodes prepared from a series of activated fluid coke samples, as shown in Table 1. Electrode films were prepared by mixing the one AC material with a polytetrafluoroethylene (PTFE) binder (Sigma Aldrich 60 wt.% suspension in water) and carbon black (CB) (used as supplied by Fisher Scientific), which was used as a conductive additive. The following dry mass mixture was applied to all electrodes; 90 wt.% AC, 6 wt.% CB and 4 wt.% PTFE.

The disc electrodes were then dried at 110 °C for 4 h. As shown in Fig. 1, a two-electrode cell was constructed using the dried composite disk electrodes mounted on nickel mesh current collectors and separated by a polyphenylene sulphide polymer separator. The two-electrode test cell was compressed using poly(methyl methacrylate) plates and stainless steel bolts. The resulting cell was then soaked in 4 M potassium hydroxide electrolyte for a minimum of 7 days prior to testing. The electrochemical performance was characterized using cyclic voltammetry and galvanostatic cycling using a Solartron 1280B/C potentiostat.

3. Results and discussion

3.1. Surface area and pore size distribution

The specific surface area and specific pore volume of the various AFC samples, the raw OSFC sample and the CSAC are listed in Table 2. These data show that the specific surface area and specific pore volume of the initial fluid coke sample was increased significantly during the activation process, with increases in both the mesopore and micropore surface area and pore volume. These results confirm that potassium hydroxide chemical activation is an effective method to greatly increase the porosity of carbonaceous OSFC. While the four AFC samples show some variability in their respective specific surface areas and pore volumes, the micropore fraction based on specific surface area and specific pore volume is consistent for all AFC samples, as shown in Table 2.

A comparison between the AFC materials and the CSAC materials shows that the activated fluid coke samples have a larger specific surface area and specific pore volume. In addition, the micropore fractions of the AFC samples are different from the CSAC; the coconut shell-derived AC has a higher fraction of both surface area and pore volume associated with micropores.

In literature, the reported specific surface area of coal and coke derived AC samples range between 1500 $m^2\ g^{-1}$ and 3500 $m^2\ g^{-1}$ depending on the activation technique and conditions [2,3,7,15,16]. The AFC samples used in the current study have by comparison moderate specific surface area values; however, the large mesopore fraction allows for improved ion diffusion in the pores compared to purely microporous materials.

The nitrogen adsorption and desorption isotherms for the activated fluid coke samples, as received oil sands fluid coke, and the commercial coconut shell activated carbon sample are displayed in Fig. 2(a), and the carbon dioxide adsorption isotherms are displayed in Fig. 2(b). When comparing the nitrogen adsorption and desorption isotherms minimal hysteresis is observed, indicating that the porous carbon samples adsorb and desorb at similar rates and that there are minimal bottleneck-type pore shapes. The activated fluid coke samples have very large adsorption volumes compared to both the coconut shell activated carbon and the oil sands fluid coke. As well, the oil sands fluid coke has a very low

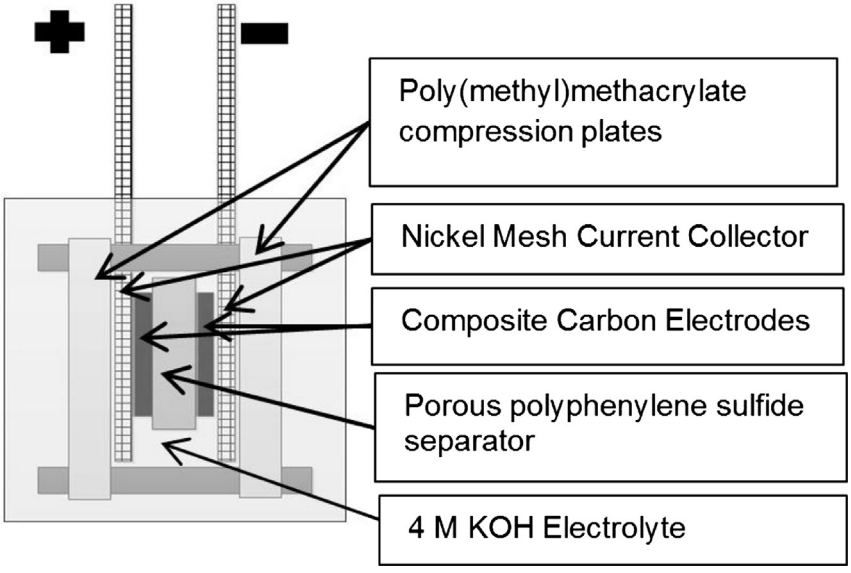

Fig. 1. Schematic of EDLC two-electrode test cell.

Table 2
Specific surface area (SSA) and specific pore volume (SPV) of the activated carbon samples prepared from fluid petroleum coke (AFC) and commercial coconut shell AC (CSAC) and the raw material, oil sands fluid coke (OSFC).

	Total SSA ($m^2\ g^{-1}$)	Micropore fraction	Total SPV ($cm^3\ g^{-1}$)	Micropore fraction
AFC-1	1776	0.75	0.893	0.55
AFC-2	1632	0.74	0.830	0.54
AFC-3	1957	0.71	0.992	0.53
AFC-4	1764	0.73	0.907	0.50
CSAC	1126	0.87	0.490	0.65
OSFC	232	0.94	0.079	0.73

nitrogen adsorption volume confirming the low specific surface area and pore volume.

The nitrogen isotherms follow both Type I adsorption isotherms for microporous materials and Type II isotherms for mesoporous materials. The activated fluid coke samples have combined Type I and Type II isotherms indicating there is a mixture of micropores, indicated by Type 1 isotherms, and larger mesopores, indicated by Type II isotherms. This observation is further confirmed by the surface area distribution, with approximately 70–75% of the total surface area contributed by micropores and 25–30% as a result of mesopores. In contrast, the CSAC material shows ideal Type I isotherm behaviour, with almost no hysteresis, indicating a highly microporous material. Again, this is confirmed with the pore size distribution showing 87% of the total SSA is a result of micropores.

The carbon dioxide adsorption isotherms displayed in Fig. 2(b) show the relative importance of sub-nanometer diameter pores in the materials. The results are comparable with the relative microporous SSA values of each material.

Both the nitrogen and carbon dioxide isotherm results and the specific surface area, pore volume, and pore size distribution fit with the comparative microporous and mesoporous surface areas.

The pore size distributions (PSDs), based on pore volumes, of the AFC samples are shown in Fig. 3. As shown, all of the activated coke samples have similar pore size distributions and volumes in the sub-nanometer range ($d < 1$ nm); however differences are observed in the relative distribution of the larger micropores (1–2 nm) and the smaller mesopores (2–10 nm). As these latter sized pores affect ion transport within the porous carbon structure, the differences in mesopore distribution may potentially affect the electrochemical performance of these AC materials. As shown in Fig. 3, the major differences in the activated coke samples occur in the 1.0–1.5 nm pore range and the 2.0–3.5 nm pore range.

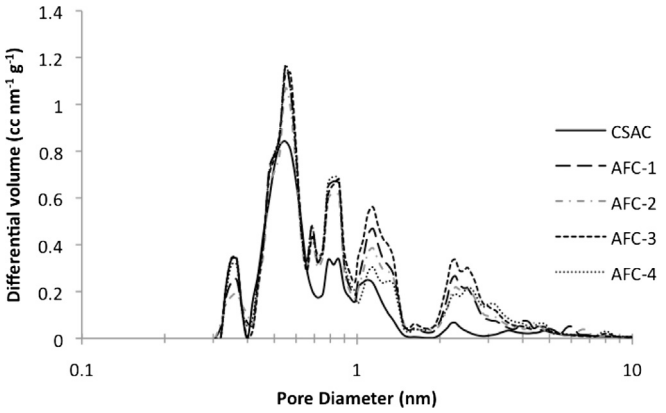

Fig. 3. Pore size distribution of AFC and CSAC samples using combined CO_2 and N_2 DFT analysis.

The commercial CSAC sample has a similar distribution of pore sizes in the sub-nanometer pores; however, the volume of these pores is lower than the activated coke samples. Compared to the activated coke, the CSAC has a different pore size distribution and a lower volume and surface area associated with pores greater than 1 nm in diameter.

3.2. Particle structure imaging

Scanning electron microscopy (SEM) imaging was performed on the as-received raw fluid petroleum coke and the activated fluid coke (AFC-3). A typical raw fluid coke particle is displayed in Fig. 4(a); it is nearly spherical in shape with many rather smooth surface irregularities that seem to show how the particle grows spherically outwards. By comparison the activated coke particle, shown in Fig. 4(b), has a more fractured surface structure with multidirectional cracks (up to approx.30 μm in depth), which are the result of the activation process. Another distinguishing feature of activated fluid coke is its uniquely layered structure as seen in Fig. 4(c), due to the coking process. The fluid coking process, which entails repeated cycling of the coke particles through the reactor, is responsible for the layered morphology with each layer ranging in thickness from between 1 and 6 μm. The layered, fractured structure contributes to the higher surface area reported for the activated fluid coke. Further, it is hypothesized that this irregular layered structure improves AFC's performance by enabling more

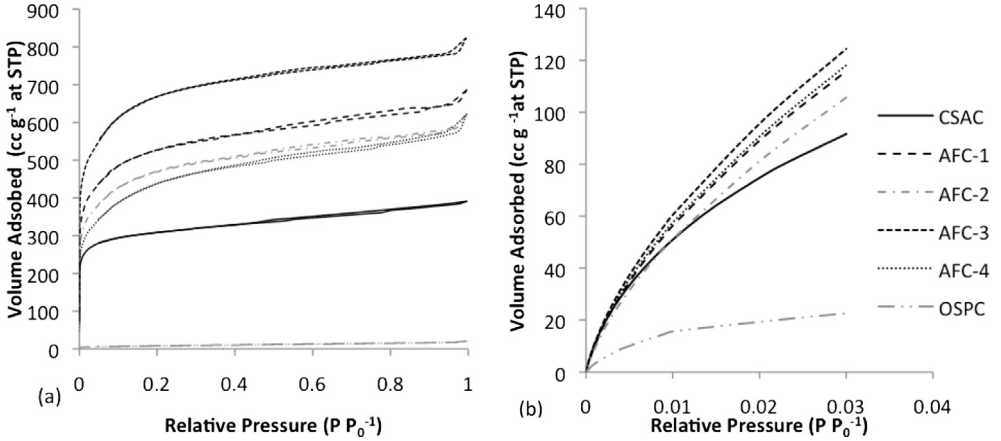

Fig. 2. Nitrogen (a) and carbon dioxide (b) isotherm adsorption and desorption results for activated fluid coke samples, the commercial coconut shell AC, and the as received oil sands fluid coke.

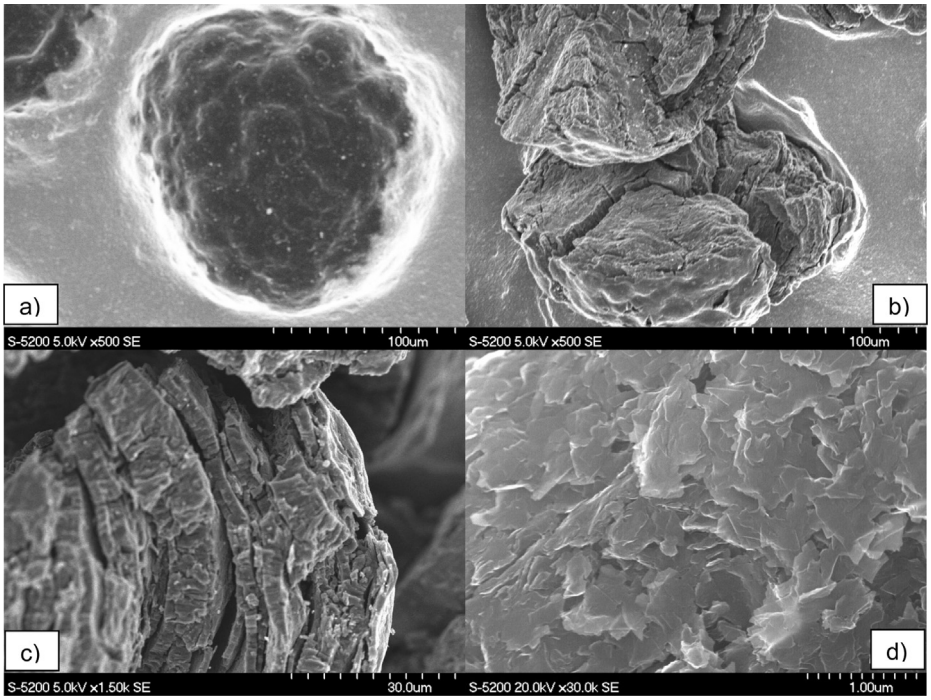

Fig. 4. SEM images of raw fluid coke and activated fluid coke (AFC-3). Image a) shows a raw fluid coke particle prior to activation, image b) illustrates the complete particles of activated fluid coke, while image c) illustrate the macroscopic layered structure of the edge of the upper activated fluid coke particle and image d) illustrates the microscopic layered structure of the activated fluid coke.

effective ion diffusion into and out of the internal structure of the activated fluid coke during charging/discharging sequences.

The microscale features of the activated fluid coke surface are displayed in Fig. 4(d). The surface of the activated coke is composed of non-uniform, multi-directional carbon layers. The edges of the layers appear to be fractured and do not form an ordered structure on the surface of the particle. Again, this layering is expected to increase the total surface area and provide effective channels for ion adsorption/desorption in energy charging/discharging.

3.3. Carbon content and chemical composition

The high carbon content of the AFC samples shown in Table 3 indicates that the AC derived from fluid coke should have good electrochemical performance, due to the high conductivity and chemical stability of the carbon [1,4].

Based on elemental composition, the major difference between the activated fluid coke and the coconut shell derived AC material is the sulphur content. Prior to carbonization, coconut shells have less than 0.5 wt.% sulphur which leads to a very low sulphur content in the resulting activated material [25]. In contrast, the OSFC has an initial average sulphur content of 6.6 wt.% [19], which decreases to approximately 2.5 wt.% in the activated samples.

Table 3
Ultimate analysis of activated carbon materials in weight percentage.

Sample	C	H	N	S
AFC-1	93.5 ± 1.26	0.6 ± 0.06	0.4 ± 0.09	2.4 ± 0.15
AFC-2	88.0 ± 0.40	0.6 ± 0.02	0.4 ± 0.04	2.4 ± 0.13
AFC-3	91.1 ± 1.50	0.5 ± 0.06	0.3 ± 0.02	2.5 ± 0.20
AFC-4	92.1 ± 0.52	0.7 ± 0.10	0.3 ± 0.01	2.6 ± 0.10
CSAC	92.2 ± 0.27	0.9 ± 0.02	0.4 ± 0.04	–
OSFC[a]	82.0 ± 1.26	1.7 ± 0.08	1.8 ± 0.15	6.6 ± 0.27

[a] Taken from Furimsky [19].

3.4. Electrochemical performance

The activated coke samples had ideal double layer capacitive behaviour, based on the two-electrode cyclic voltammograms (CVs) displayed in Fig. 5. The CVs are rectangular in shape, indicating low equivalent series resistance. As well, there are no distinct voltage dependent charge transfer reaction peaks present. Therefore, the activated fluid coke displays ideal behaviour for EDLC energy storage. The electrochemical performance of the AFC and CSAC samples is compared in Table 4. The AFC samples demonstrate a high capacitance when normalized to both weight and surface area of AC in the disc electrode. The gravimetric capacitance of the AFC materials is more than double that of the CSAC used in this study. Compared to the commercial CSAC, the coke derived AC samples all have a higher capacitance and energy density and comparable equivalent series resistance. Therefore, it can be concluded that the activated fluid coke demonstrates good electrochemical performance compared to the CSAC.

The AFC samples have high specific capacitances values, which suggest that the electrolyte ions are able to penetrate a large portion of the total specific surface area. The specific capacitance is 30–40% greater than the commercial CSAC sample used in this study. The higher specific capacitance of the AFC samples, compared to that of the CSAC, indicates that the pore size distribution and network structure is more ideally suited for ion transport to internal surface structures, thereby resulting in an increased ion storage in the AFC electrodes. This may be associated with the layered carbon structure, as observed in the SEM images above. This structure allows for easier ion access into the internal AC's particle structure, as the spacing between the layers is large compared to the ion sizes. However, as observed in Table 4, the specific capacitance of the activated coke samples is still less than the generally accepted theoretical values for planar graphene carbon sheets, estimated as 21 $\mu F\ cm^{-1}$ [5,17]. Thus, there remains surface area that has not been accessed by ions during charging. As

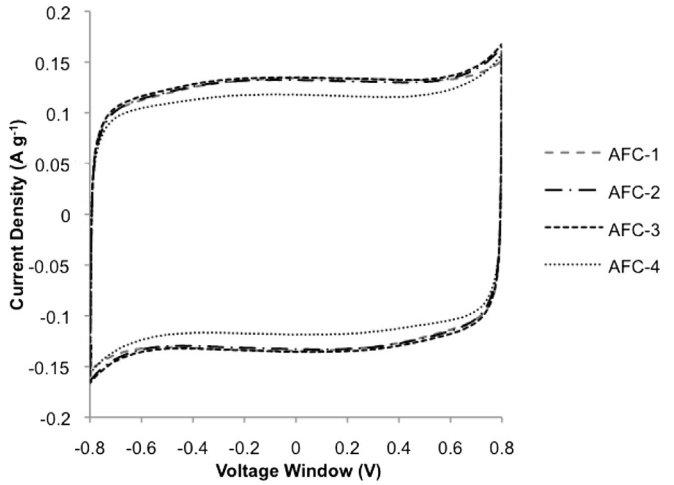

Fig. 5. Cyclic voltammograms of activated fluid coke samples (AFC) at 1 mV s^{-1} sweep rate, showing ideal rectangular shape.

a result, there is additional accessible surface area and thus untapped energy storage capacity.

The energy storage of the activated fluid coke material may also be enhanced due to the presence of sulphur compounds in the carbon structure. The presence of sulphur compounds in the activated fluid coke may lead to enhanced energy storage due to improved wettability and potential charge transfer reactions. In recent literature, the presence of sulphur functional groups in carbon materials has been shown to results in a potential increase in capacitance due to charge transfer reactions, in both acidic and alkaline electrolytes [26,27]. However, there remains a gap in the understanding of sulphur based pseudocapacitance and the required concentration and functionalization of sulphur groups on the surface to greatly enhance the capacitance.

The oil sands fluid coke is a unique carbon material due to the presence of organic sulphur species within the carbon structure, making the sulphur impurities more stable. Characterization of sulphur species is difficult due to the wide variety of oxidation states and speciation. Previous research by Cai et al. indicates that oil sands fluid coke has a large fraction of reduced sulphur species, such as sulphide, disulphide, thiol, and thiophene groups, all of which involve organic sulphur bonds to carbon atoms. Using X-ray photoelectron spectroscopy (XPS), Cai et al. estimated that in oil sands fluid coke 91% of the total sulphur is in a reduced form (sulphide, thiol, thiophene), and 9% is oxidized sulphur, in the forms of sulphoxide and sulphate. This study also demonstrated that activation with potassium hydroxide and sulphur dioxide, performed by Cai et al., resulted in conversion of some of the reduced sulphur species to oxidized sulphur species, which would be expected due to the oxidizing nature of potassium hydroxide and sulphur dioxide [28]. Reduced sulphur species would behave similarly to oxygen species, with two covalent bonds to carbon, and two lone pairs (4 electrons), which could enhance adsorption affinity of electrolyte ions. Oxidized sulphur has the potential to participate in charge transfer reactions due to the high electron density of the species as outlined in Refs. [26,27].

The activated fluid coke has moderate sulphur content (~2.5 wt. %); therefore, though the sulphur heteroatoms may contribute additional energy storage capabilities, it is unlikely that the sulphur heteroatoms are solely responsible for the enhanced specific capacitance. Further investigation into the effects of the potential sulphur-related enhancement in capacitance is required.

In summary, the activated coke samples have high specific capacitance values, comparable with other promising activated carbon samples reported in the literature [1–3].

Table 4
Specific surface area (SSA) and electrochemical performance of AFC and CSAC samples in 4 M KOH electrolyte, using a sweep rate of 1 mV s^{-1} and a voltage window of 0.8 V.

Sample	Total SSA (m^2 g^{-1})	Single electrode capacitance		ESR (Ω)	2-Electrode energy density (Wh kg^{-1})
		(F g^{-1})	(μF cm^{-1})		
AFC-1	1776	256	14.4	0.49	11
AFC-2	1632	253	15.5	0.52	11
AFC-3	1957	257	13.2	0.50	11
AFC-4	1764	228	12.9	0.60	10
CSAC	1126	116	10.3	0.56	5

3.4.1. Effect of charging current on capacitance

Another key factor that is considered when evaluating AC material for EDLC applications is the performance at higher charging rates. One of the limitations of AC based EDLCs is the complex porous structure and ion transport within a confined structure. The ionic resistance associated with diffusion in the confined pores leads to an observed decrease in capacitance as charging rate is increased. Depending on the electrolyte, the operating conditions, and the initial and final current density or sweep rate, the capacitance decreases ranged from 20% to greater than 50% [1,3,10,15,29,30]. It has been demonstrated that AC electrodes may be charged at a high current density; however, there is a trade-off between high capacitance and short charging time.

The relationship between capacitance and current density or sweep rate for the AFC electrodes is displayed in Fig. 6(a) and (b), respectively. The capacitance of both the CSAC and the AFC materials decreases as current and sweep rate increase, as expected. The activated coke samples have a high capacitance at higher current densities, with a capacitance decreases between 28% and 35% as the current density increases from 25 mA g^{-1} to 7500 mA g^{-1}. The AFC materials continue to outperform the CSAC, which has a decrease in capacitance of 39% as the current density is increased from 25 mA g^{-1} to 7500 mA g^{-1}. Furthermore, the capacitance at the higher charging rates remains high for the AFC materials. At the fast charging rates, the capacitance remains above 160 F g^{-1} for all the activated coke samples.

Torchala et al. have demonstrated high rate capability with activated mesobeads, as the current is increased from 200 mA g^{-1} to 5000 mA g^{-1} a low capacitance decrease was observed, between 12 and 20% [2]. Over a similar range, 250 mA g^{-1} to 5000 mA g^{-1} the activated fluid coke samples, AFC-1, AFC-2, and AFC-3, have similar capacitance decreases of 18%. The AFC-4 sample has a slightly higher decease in capacitance of 21% over the same current density window.

As the charging rate is increased, the specific capacitance decreases for all materials. The decrease in specific capacitance demonstrates that as the current density increases, access to the internal pore structure is limited and a lower portion of the total specific surface area is used for energy storage.

The behaviour of the CSAC and AFC samples with varying sweep rate differs from the effect of current density. As the sweep rate increases to 250 mV s^{-1} and 500 mV s^{-1}, the capacitance of all materials is similar (~45–60 F g^{-1} and 20–30 F g^{-1}, respectively); however, at slower sweep rates, the capacitance of the activated coke samples is significantly greater compared to that of the CSAC material. Therefore, these results suggest that at very high charging rates, ion diffusion into the porous carbon is limited by the short charging times. It should be noted that the charging times for the

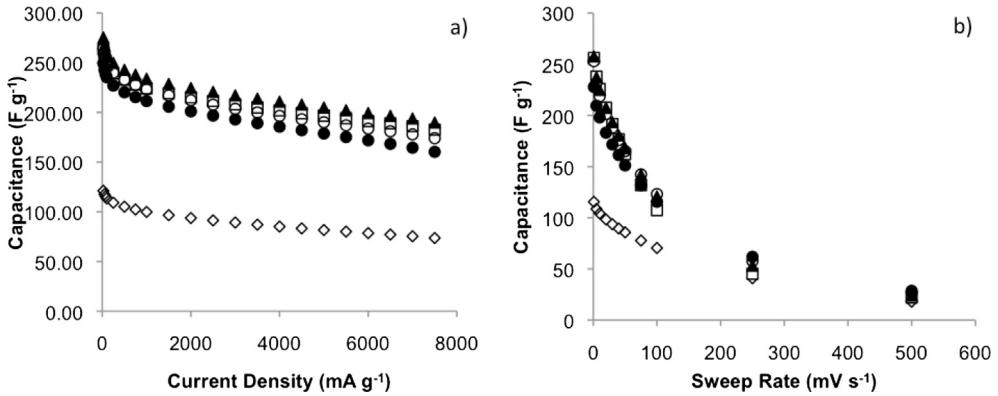

Fig. 6. Relationship between capacitance and charging rate for a) charging current density for galvanostatic cycle testing, and b) sweep rate for cyclic voltammetry. CSAC (◊), AFC-1 (▫), AFC-2 (○) AFC-3 (▲), AFC-4 (●).

highest sweep rate is much shorter than the highest current density.

Overall, the commercial coconut shell AC has a lower capacitance and a more rapid decrease in capacitance when compared to the activated coke samples' results. In the CSAC, the pore volumes associated with pores of diameters 1.0–1.5 nm and 2.0–3.5 nm are less than the coke samples, which suggests that these pores ranges may be critical for ion transport. Therefore, the pore network and layered carbon structure of the activated fluid coke may allow for more ion mobility and easier diffusion within the internal structure of the porous carbon.

3.4.2. Energy and power density of activated fluid coke

The Ragone plot for the two-electrode cell is displayed in Fig. 7 for the activated coke samples compared to the commercial coconut shell AC and literature samples of graphene [12], and vertically aligned carbon nanotubes, and carbon nanoribbons [31] electrodes. The best performing and the worst performing activated fluid coke samples (AFC-3 and AFC-4, respectively) are presented for clarity. The activated coke shows high energy storage in the device setup per kilogram of activated material compared to that of the commercial AC. However, though the energy storage of the AFC is higher, the power density of both AC materials is comparable; therefore, the energy storage has been increased without compromising the power capabilities of the device. The activated fluid coke has comparable energy density and power density compared to the graphene electrode sample, which was an activated carbon and graphene composite electrode of a weight ratio of 3:1 [12]. The AFC samples have a higher energy density to the carbon nanotube electrodes; however, the power density of the carbon nanotube electrodes is considerably greater than that of the activated coke. Compared to the nanoribbons created from the carbon nanotubes, the AFC samples have higher energy density, but considerably lower power density, with the power density of the nanoribbons reaching 103 kW kg^{-1}.

These results suggest that the activated coke samples have an improved capacitance and energy storage ability compared to a commercial AC, CSAC. The increase in capacitance is greater than the increase in surface area, indicating that the high capacitance of the AFC is a result of chemical or structural properties. As well, the activated fluid coke has a higher fraction of retained capacitance at higher current densities, compared to the CSAC. The two key differences in the samples are: 1) the pore size distribution, and 2) the chemical composition of the ACs.

Comparing with CNTs, graphene, and nanoribbons, activated fluid coke has a comparable or higher energy density. However, the power density of the activated carbon materials is less that the nanotubes and nanoribbons. The higher energy density of the AFC materials is associated with the high surface area, the layered structure of the samples and potentially associated with the sulphur impurities, as discussed above. While the lower power density is a result of the highly ordered structure of CNTs and nanoribbons [31], allowing for easier ion diffusion into and out of the pores.

These results suggest that high performing ACs for electrochemical applications require a balance of micropores and mesopores. The large amount of micropores results in higher surface area, allowing for increases in capacitance; however, it is critical to have a mesoporous network to allow ion transport. The activated coke samples appear to have a good combination of mesopores and micropores to allow ion diffusion into the internal structure and improved specific capacitance at both low and high current densities.

Further research is required to substantiate these results, in which additional activated coke samples will be prepared to investigate the effect of increasing micropores, or mesopores. As

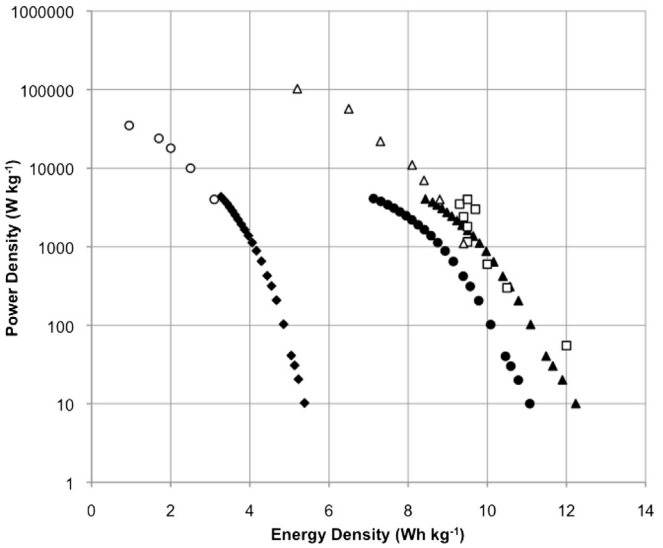

Fig. 7. Ragone Plot of device energy and power density comparing the activated coke (AFC-3) and activated coke (AFC-4) (AFC-3 (▲), AFC-4 (●)) samples to coconut shell derived-AC (CSAC) (◆) and selected points for literature data for carbon nanoribbons (△) [31] and vertically aligned carbon nanotubes (○) [31] and graphene oxide [12] (□) electrodes.

well, the effects associated with the differing chemical composition, primarily sulphur content, of the activated fluid coke compared to biomass-derived ACs will be further investigated.

4. Conclusion

Activated fluid coke (AFC) presents a unique opportunity to generate AC for electrochemical applications from a waste product. The results from this work confirm that the AFC electrodes have a high capacitance and show good performance at high charging currents, with a capacitance at 7500 mA g^{-1} of greater than 160 F g^{-1}. When compared with commercial AC prepared from coconut shells (CSAC), the activated coke samples have a higher surface area and a higher capacitance, as well as better performance at higher current densities. As well, the activated fluid coke derived AC demonstrates the performance that is comparable with other top performing AC materials reported in published literature.

From an environmental perspective, the activated oil sands fluid coke presents a unique opportunity to re-use an environmentally harmful by-product for energy storage applications.

Acknowledgements

The authors would like to acknowledge the National Science and Engineering Research Council (NSERC) (453859), the Consortium on Sustainable Materials (COSM-Japan) (481535) and the Chinese-NSF (51174150) for funding for this project. As well, the authors would like to thank the Canadian Oil Sands Industry for supply of raw petroleum fluid coke.

References

[1] M. Inagaki, H. Konno, O. Tanaike, J. Power Sources 195 (2010) 7880–7903.
[2] K. Torchala, K. Kierzek, J. Machnikowski, Electrochim. Acta 86 (2012) 260–267.
[3] L. Wang, J. Wang, F. Jia, C. Wang, M. Chen, J. Mater. Chem. A 1 (2013) 9498–9507.
[4] R. Kotz, M. Carlen, Electrochim. Acta 45 (2000) 2483–2498.
[5] B.E. Conway, Kluwer Academic, Ottawa, 1999.
[6] A. Burke, J. Power Sources 91 (2000) 37–50.
[7] A. Ghosh, Y.H. Lee, ChemSusChem 5 (2012) 480–499.
[8] J. Chmiola, G. Yushin, R. Dash, Y. Gogotsi, J. Power Sources 158 (2006) 765–772.
[9] Y. Yamada, O. Kimizuka, O. Tanaike, K. Machida, S. Suematsu, K. Tamamitsu, S. Saeki, H. Hatori, Electrochem. Solid State Lett. 12 (2009) K14–K16.
[10] M. Lazzari, F. Soavi, M. Mastragostino, Fuel Cells 10 (2010) 840–847.
[11] M. Meyyappan, J. Vac. Sci. Technol. A 31 (2013) 14.
[12] L. Jiang, J.W. Yan, Y. Zhou, L.X. Hao, R. Xue, B.L. Yi, J. Solid State Electrochem. 17 (2013) 2949–2958.
[13] J. Yan, J.P. Liu, Z.J. Fan, T. Wei, L.J. Zhang, Carbon 50 (2012) 2179–2188.
[14] M.D. Stoller, S.J. Park, Y.W. Zhu, J.H. An, R.S. Ruoff, Nano Lett. 8 (2008) 3498–3502.
[15] A. Alonso, V. Ruiz, C. Blanco, R. Santamaria, M. Granda, R. Menendez, S.G.E. de Jager, Carbon 44 (2006) 441–446.
[16] K. Kierzek, E. Frackowiak, G. Lota, G. Gryglewicz, J. Machnikowski, Electrochim. Acta 49 (2004) 515–523.
[17] J.L. Xia, F. Chen, J.H. Li, N.J. Tao, Nat. Nanotechnol. 4 (2009) 505–509.
[18] R. DiPanfilo, N.O. Egiebor, Fuel Process. Technol. 46 (1996) 157–169.
[19] E. Furimsky, Fuel Process. Technol. 56 (1998) 263–290.
[20] M. Teare, A. Burrowes, C. Baturin-Pollock, D. Rokosh, C. Evans, R. Marsh, B. Ashrafi, C. Tamblyn, S. Ito, A. Willwerth, M. Yemane, J. Fong, M. Kirsch, C. Crowfoot, 2013.
[21] I.V. Bylina, S. Tong, C.Q. Jia, J. Therm. Anal. Calorim. 96 (2009) 91–98.
[22] M.J. Yuan, S.T. Tong, S.Q. Zhao, C.Q. Jia, J. Hazard. Mater. 181 (2010) 1115–1120.
[23] C.C. Small, Z. Hashisho, A.C. Ulrich, Fuel 92 (2012) 69–76.
[24] J.N. Caguiat, D.W. Kirk, C.Q. Jia, Carbon 72 (2014) 47–56.
[25] E. Ganapathy Sundaram, E. Natarajan, J. Eng. Res. 6 (2009) 33–39.
[26] M. Seredych, T.J. Bandosz, J. Mater. Chem. A 1 (2013) 11717–11727.
[27] W.T. Gu, M. Sevilla, A. Magasinski, A.B. Fuertes, G. Yushin, Energy Environ. Sci. 6 (2013) 2465–2476.
[28] J.H. Cai, E. Morris, C.Q. Jia, J. Sulfur Chem. 30 (2009) 555–569.
[29] J. Chmiola, G. Yushin, Y. Gogotsi, C. Portet, P. Simon, P.L. Taberna, Science 313 (2006) 1760–1763.
[30] H. Chen, F. Wang, S. Tong, S. Guo, X. Pan, Appl. Surf. Sci. 258 (2012) 6097–6102.
[31] C.G. Zhang, Z.W. Peng, J. Lin, Y. Zhu, G.D. Ruan, C.C. Hwang, W. Lu, R.H. Hauge, J.M. Tour, ACS Nano 7 (2013) 5151–5159.